Instituto Nacional de Investigación y Tecnología Agraria y Alimentaria (INIA)
http://dx.doi.org/10.5424/sjar/2014124-5766

Spanish Journal of Agricultural Research 2014 12(4): 941-951
ISSN: 1695-971X
eISSN: 2171-9292

RESEARCH ARTICLE

OPEN ACCESS

Soil-blade orientation effect on tillage forces determined by 3D finite element models

Ayadi Ibrahmi[1,2]*, Hatem Bentaher[1,2] and Aref Maalej[2]

[1] *Higher Institute of Industrial Systems (ISSIG). Gabes, Tunisia.* [2] *LASEM Laboratory. National Engineer's School of Sfax (ENIS). PBW. University of Sfax. 3000 Sfax, Tunisia*

Abstract

This paper investigated the effect of the cutting parameters of a blade on the tillage force components using finite element modeling. A three-dimensional model was carried out with Abaqus Explicit in order to study the interaction between the tool and soil. The soil was modeled with linear forms of the Drucker-Pager model, while the tool was considered as a rigid body with a reference point taken at its tip. The effect of tillage depth and the width of a vertical blade were studied. It was found that the amounts of the draught and vertical forces increase linearly with a slope of 0.037 and 0.0143 respectively when the width increases. The narrow tool (width < 60mm) has a greater effect on the specific draught force than a larger tool. Draught and specific draught force increase with polynomial and linear curve respectively versus the depth. However, this effect was reduced for the vertical force. These results were in a good agreement with previously published works. The second part of this paper is focused on the oblique position of the blade to evaluate the effect of the attack angles on both the tillage forces (draught, lateral and vertical) and the cutting process of the soil during and after its failure. For all considered angles, the draught force presents the highest values compared to the vertical and lateral forces. Results showed that working with small cutting and an average rake angles (30° to 60° and 45° respectively) can produce a good soil inversion.

Additional key words: FEM; oblique blade; force; attack angles.

Introduction

Tillage is a necessary action on soil to prepare favorable conditions for plant growth. Such an action is costly and time consuming during the production cycle. For this reason tillage power optimization is still one of the main research fields (Collins *et al.*, 1978; Bloome *et al.*, 1983; Singh *et al.*, 1991; Owend & Eward, 1996). Some studies have already started this optimization either by reducing the tillage frequency (number of operations during the production cycle) (Temesgen *et al.*, 2008) or by using strip tillage (limiting the surface of tillage) (Mullins *et al.,* 1998; Licht & Al-Kaisi, 2005; Temesgen *et al.*, 2012; Celik *et al.*, 2013; Trevini *et al.*, 2013). However, these techniques are acceptable in very few conditions and cannot be generalized especially with hard environmental conditions (scarcity of water and arid climate).

Other researchers have worked on the optimization of the tillage process by reducing the tillage forces. To identify these forces three approaches (analytical, empirical and numerical methods) have been suggested. The analytical approaches were based on the lateral earth pressure theory. They achieved some original empirical findings that were validated experimentally (McKyes & Ali, 1977; McKyes & Desir, 1984; Gupta *et al.*, 1989; Tong & Moayad, 2006).

With the development of computer science, numerical methods have been used to study the interaction between the soil and cutting tools. This approach helped understand the tillage phenomena and to predict induced forces. Studies carried out with this approach can be classified into three categories: discrete element method (DEM), computational fluid dynamics (CFD) and finite element method (FEM). In DEM the soil is considered as an assembly of individual granu-

* Corresponding author: ayadi.ibrahmi@yahoo.fr; ayadiibrahmi@hotmail.fr
Received: 16-02-14. Accepted: 10-10-14.

Abbreviations used: CFD (computational fluid dynamics); DEM (discrete element method); FEM (finite element method); RF (reaction force); RF2 (vertical force); RF3 (draught force); α (cutting angle); θ (rake angle).

les and each one interacts with its neighboring granules under external forces, such as tillage action. Forces arise at the contact points between granules, causing their displacements. The contact force is also determined by the particle properties (*e.g.* stiffness) and the overlap between the granules in contact (Momozu *et al.*, 2003; Shmulevich *et al.*, 2007; Franco *et al.*, 2007; Obermayr *et al.*, 2011; Chen *et al.*, 2013). For CFD the tool is considered to be stationary and the soil (visco-plastic fluid) was displaced around the tool. This technique is based on the finite volume method and involved in solving Navier-Stokes equations for incompressible laminar flows (Karmakar & Kushwaha, 2005; Karmakar *et al.*, 2007, 2009). In the third approach (FEM), the soil is supposed to be a continuous material with different behavior models (hypoplastic, elastic, perfectly plastic, Drucker Prager...), and the tool is considered to be a rigid part. Indeed the first research papers treated the problems in two dimensions for simple plane tools (Yong & Hanna, 1977; Fielke, 1999; Davoudi *et al.*, 2008). This approach was used for the problems in three dimensions with more complicated shapes (Chi & Kushwaha, 1987, 1988; Mouazen & Nemenyi, 1999; Abo-Elnor *et al.*, 2004; Bentaher *et al.*, 2013).

The main purpose of our work was to study the effect of the operational conditions of a simple tool (blade) and to evaluate the influence of its attack angles (cutting and rake angles) on the tillage force components. To study the influence of the blade width, depth, and orientation relative to the soil box a three dimensional FEM using Abaqus Explicit was used. The implementation of this explicit model was achieved through several steps using this software. A focus on the cutting soil in front of the tillage tool was made to understand the effect of the studied angles on the soil behavior during and after its failure.

Material and methods

The soil failure depends mainly on its physical and mechanical properties, the tool shape and working parameters such as cutting speed and operating depth.

Soil model

The soil environment is influenced by the state of three soil phases (solid, liquid and gaseous) and by a complex equilibrium among them, within which a number of different physical and chemical processes control the mechanical behavior of the soil (Richards & Peth, 2009). The mechanical property of soil in loading and unloading presents an elastic and plastic deformation with a nonlinear variation (Upadhyaya *et al.*, 2002).The comprehensive expression of the stress-strain behavior of agricultural soils is complex and difficult to describe with a simple relationship. Specifically, the identification of the model parameters such as elastic properties, yield surface, hardening law, plastic potential, and flow rule are compulsory to carry out the mathematical formulation of the stress-strain relationship for an elastic-plastic material under general loading conditions. Indeed, several previous scientists tried to find out whether the plasticity theory is applicable to soil mechanics in both civil engineering and tillage (Zhang, 1993; Li, 2004). A number of criteria like Mohr-Coulomb, Drucker-Prager and Cam-Clay have been used for the simulation of problems in soil mechanics (Bose & Som, 1998; Fielke, 1999; Mouazen & Nemenyi, 1999; Ucgul *et al.*, 2014).

The Drucker-Pager model and its extended form are used to simulate the soil and rock behavior specifically where material yield is associated with hardening. Different forms of yield surfaces can be found in the Drucker-Pager model. It can have linear, hyperbolic, or general exponential forms (Abaqus, 2010). In this study, the soil was considered as an elastic-plastic continuum that reveals material hardening. So, the yield criterion was defined using the linear form of the extended Drucker-Prager material model with a hardening property.

The linear Drucker-Pager criterion is written as:

$$F = t - p \cdot \tan(\beta) - d \qquad [1]$$

where F = the yield function, t = the deviatoric stress given by Eq. [3]; p = the normal stress given by Eq. [2], β = the Drucker–Prager internal angle of friction, and d = the cohesion of the material.

$$p = \frac{1}{3}(\sigma_1 + \sigma_2 + \sigma_3) \qquad [2]$$

$$t = \frac{1}{2} q[1 + \frac{1}{K} - (1 - \frac{1}{K})(\frac{r}{q})^3] \qquad [3]$$

where

$$q = (\sigma_1 - \sigma_3) \qquad [4]$$

$$r^3 = -(\sigma_1 - \sigma_3)^3 = -q^3 \qquad [5]$$

where K is the ratio of the yield stress in triaxial tension to the yield stress in triaxial compression ($0.778 \le K \le 1$); $K = 1$ and $t = q$ implies that the yield surface is the Von Mises circle in the deviatoric principal stress plane; σ_1,

Table 1. Soil property parameters required by the finite element method (FEM)

Parameters	Value
Density, ρ (kg m^{-3})	1,731
Young's modulus, *E* (MPa)	8.067
Poisson's ratio, ν	0.359
Friction coefficient angle, β (degree)	42
Stress ratio, *K*	1
Dilatation angle, ψ (degree)	0
Cohesion, *C* (kPa)	15.5
Soil-metal friction angle, δ (degree)	23

σ_2 and σ_3 are compressive stress in triaxial test; r is the third invariant of deviatoric stress.

In order to simulate the cutting force, the soil was defined with different parameters required by the FEM: Young's modulus (E), Poisson's ratio (ν), bulk density (ρ), yield stress ratio in triaxial tension to triaxial compression (k), the angle of friction (β), and the dilation angle (ψ) for the plastic flow. The data used for these parameters are shown in Table 1. A value of yield stress equal to 0.16 MPa was adopted.

Furthermore, damage and failure features in the property module were used to simulate the fracture of soil which causes Abaqus Explicit to remove elements from the mesh as they fail.

Finite element model

In order to determine the three components of the predicted tillage forces, a three dimensional model was developed (Fig.1a). This model consists of two distinct Abaqus parts: (i) a deformable soil box: a 2 m long, 2 m wide and 1 m deep box, used to simulate the soil material, and (ii) a rigid blade: a discrete rigid body with a width (L), positioned at a depth (d) and oriented to the box containing the soil with an angle (α) around the y axis and with an angle (θ) around the x axis. A reference node was assigned to the blade in order to apply boundary conditions.

For this study, a constant blade velocity of 1 m s^{-1} in the tillage direction was used for all the analysis. The effects of the working depth, the width of the blade and its position to the box containing the soil on the tillage forces were studied in the present work in two parts (Fig. 1a):

— Part 1: Vertical blade (α = 90°, θ = 90°): In this part, the effects of the tool width and depth on the predicted force were studied. The tested widths were 30, 60, 90, 120 and 150 mm. Here, the depth was fixed to 100 mm. To study the effect of the depth on the predicted force, a blade of 100 mm of width was used; the tested depths ranged from 50 to 250 mm with steps of 50 mm.

— Part 2: Inclined blade: In this study six cutting (α) and rake (θ) angles (15°, 30°, 45°, 60°, 75°, and 90°) were investigated. Three cases were studied: the effect of the rake angle for α = 90° and α = 45°and the effect of the cutting angle for θ = 90°. A 100 mm wide blade was fixed at a depth of 150 mm.

The rigid body (*i.e.* the blade) was meshed with a quadratic, rigid bilinear element (R3D4, a 4-node and 3 degrees of freedom per node element) in the Abaqus

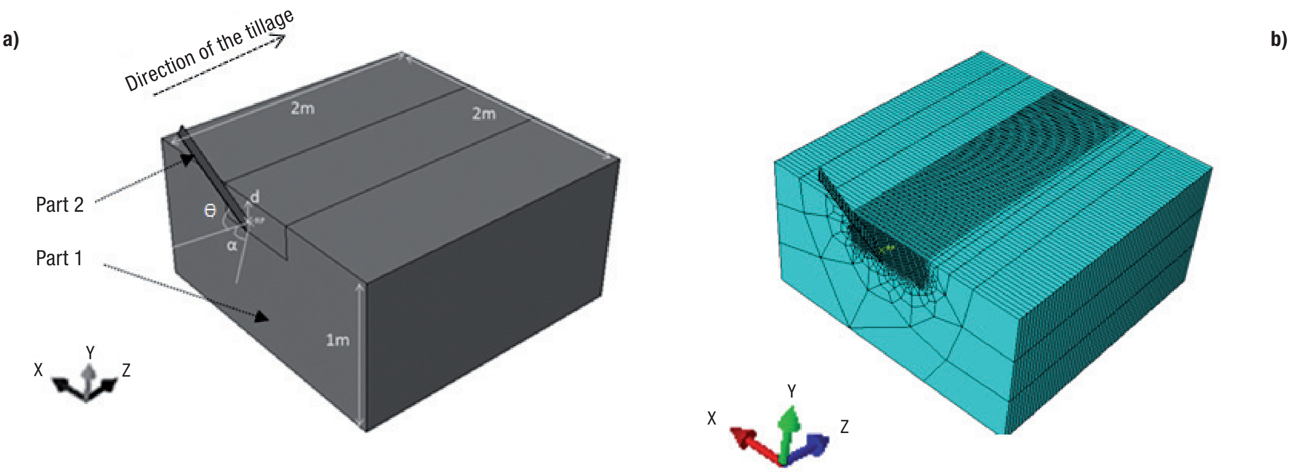

Figure 1. Three-dimensional model: soil box and blade position (a) and the finite element method (FEM) mesh of soil cutting with blade (b).

Explicit. The soil box was meshed using an 8-node linear brick, reduced integration, hourglass control (element type: C3D8R) and with a sweep meshing technique. This element type is used for 3D stress-strain analysis of continua (Abaqus, 2010).

Therefore, the soil box was partitioned into two parts. The first has a rectangle base to assign a finer mesh in a domain around the blade (Fig. 1b). The second part of the soil box was meshed coarser as it is far from the interaction zone (between the blade and the soil). The influence of the mesh size on the force was studied in a previous work (Bentaher *et al*., 2013). This partition was adopted to reduce the calculation time and to preserve a good precision of the results. The total number of nodes and elements used to describe the rigid body depends on the width of the blade.

For the boundaries condition, the soil box was fixed at its bottom and at its lateral left and right sides. The other surfaces of the soil were not constrained. In the present work, a predetermined constant translational velocity in the tillage direction (z) was imposed to the reference point of the blade. The other five degrees of freedom were fixed. The blade has to reach this speed gradually to avoid the divergence of the calculation algorithm. For this reason it was multiplied by an amplitude function V (Fig. 2).

Two steps of explicit calculus were adopted to solve this problem: an initial step in which the boundary conditions are applied, and an explicit dynamic step with a time period of 2.5 s. The model outputs were the reaction forces on the blade reference nodes. Furthermore, the outputs of interest were the soil deformations and stresses and the rigid body displacement.

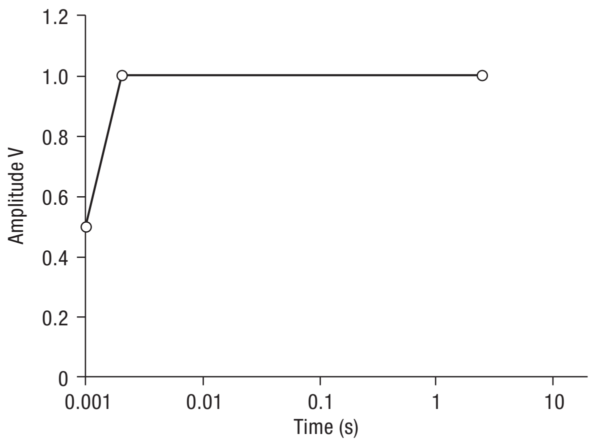

Figure 2. The amplitude function (V) modulus.

The frictional blade-soil interaction was simulated with a surface-to-surface contact law and tangential behavior. The Abaqus Explicit enforces this contact constraint using a penalty contact method, considering the contact between the soil nodes and the rigid body face in the current configuration. The friction coefficient between soil and blade was chosen equal to 0.42. With this procedure, the software automatically selects the blade as master and the deformable part (soil) as slave.

In this work, for each parameter of this study a new task was assigned to Abaqus Explicit and submitted to the solver.

Results and discussion

Vertical blade ($\alpha = 90°$, $\theta = 90°$)

Effect of the blade width

Von Mises stress contours of half the soil box and tool at different time steps are shown in Fig. 3. The zone of stress propagation is mostly concentrated in front of the blade during its displacement in the soil. The first part of the advance of the tool into the soil induced a big compression of soil until chip forming starts ($t = 0.18$ s). Once the constraint of the soil failure is reached, the soil is reversed in front of the blade. Fig. 4 shows a typical variation of the vertical and draught force calculated by the FEM without and with smoothing. These forces increase with displacement until reaching a mean value around which they oscillate. These oscillations are due to alternation between a compression phase of the soil (increasing curve), then the strain reaches the failure value and the crack propagation phase starts (decreasing part) (Fig. 5). The draught curve reaches the maximum at the beginning of the first compression phase (6 kN) and then stabilizes around a value of 5.5 kN. These results are in accordance with the published works of Shmulevich (2010), Chen *et al.* (2013), Tamas *et al.* (2013) and Bentaher *et al.* (2013). The mean value obtained after stabilization of the tillage forces, for each width, was used to draw the variation of the draught and vertical force *versus* the width. It should be noted that this method was used for all the parameters considered in the below study (depth, cutting and rake angle).

Fig. 6a shows the variation of the draught and vertical force *versus* the width. These curves show that the amounts of the draught and vertical forces increase

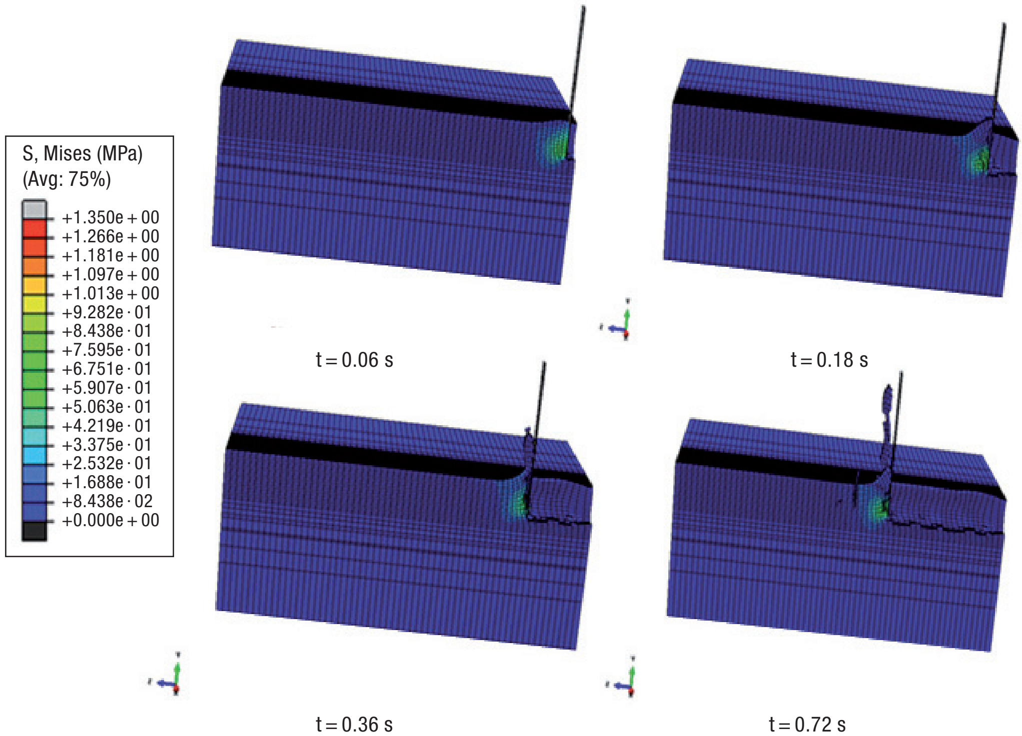

Figure 3. Von Mises stresses for different time steps.

when the width increases with a linear regression. The slope of the amount of the draught force (0.037) is near the double of the amount of the vertical one (0.0143). Considering the specific forces (force divided by the perturbed surface), the draught presents a high value for narrow tools (w < 60 mm) and it decreases asymptotically to the value of 400 kPa for larger tools (Fig. 6b).

This is in agreement with other published results (Godwin & O'Dogherty, 2007) which differentiate between wide blades and narrow to very narrow blades. In fact, the blade tillage induces a soil perturbation of two crescents on both sides of the tool. This affects the tillage draught of narrow tools by a large amount and has a reduced influence on large blades. However, the specific vertical force is independent of the width of the tool.

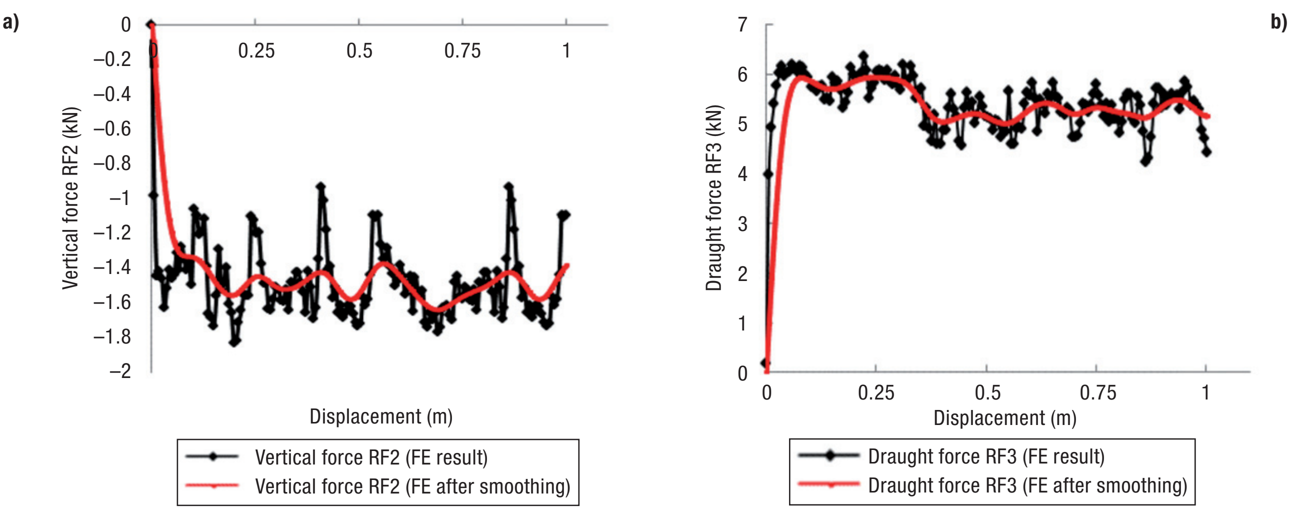

Figure 4. Typical variation of predicted tillage forces with finite element method (FEM): (a) vertical force (RF2), (b) draught force (RF3).

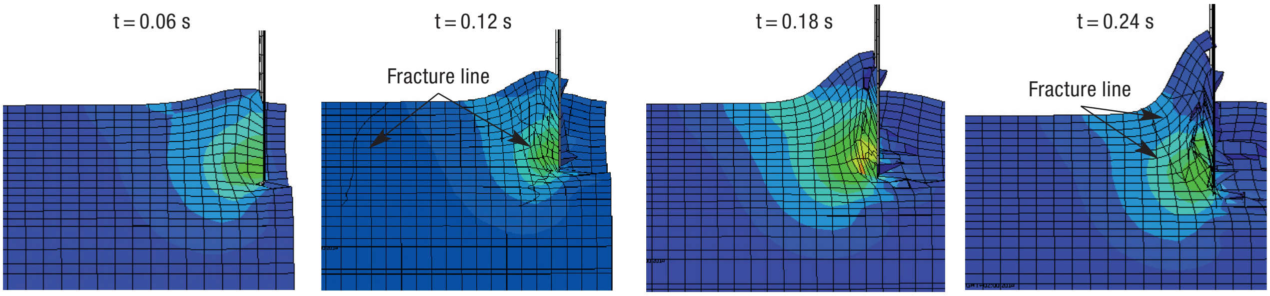

Figure 5. Alternation between two phases: compression and crack propagation.

Effect of the blade depth

Figs. 6c and 6d show the variation of the reaction and the specific forces *versus* the operating depth. These curves demonstrate that the draught force *versus* depth is best fitted to a polynomial curve of a second degree ($R^2 = 0.9999$). Specific draught force *versus* depth follows a linear curve with a slope of 1.2. The vertical force and specific vertical force are less influenced by the depth. Indeed these results are in a good agreement with the experimental results of Manuwa (2009), who explains this effect by the reason that at higher depths more soil volume is considered.

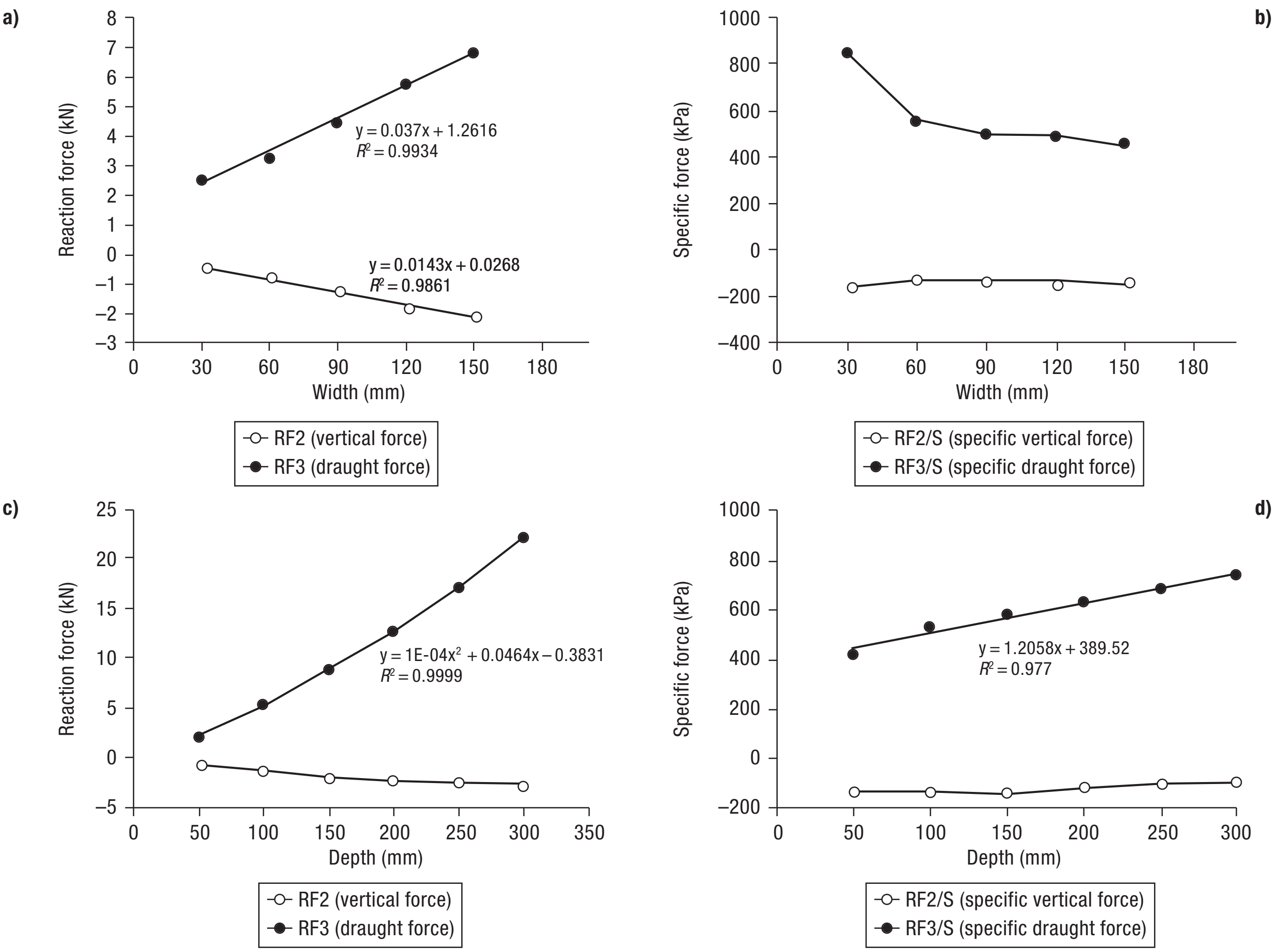

Figure 6. Effect the width and the operational depth of the blade on tillage forces (a and c respectively) and specific forces (b and d respectively).

Inclined blade

Effect of the rake angle (α = 90°)

Fig. 7 shows the cutting process for different time steps. The influence of the rake angle θ on this process is recorded. Indeed, for small angles (15 to 30°) the soil slipped onto the blade, then, for angles above 45°, the soil is reversed in front of the blade. Finally, for vertical blades (θ = 90°), the soil is compressed and fragmented. For this reason one analytical equation alone could not describe all these different cutting processes together.

Fig. 8a shows the variation of the draught and vertical force *versus* the rake angle (θ). These curves show that the draught force increases with the second degree polynomial variation of the rake angle ($R^2 = 0.99$). The best fitted curve for the vertical force is a linear variation with a correlation coefficient of 0.977. The vertical force is the result of a competition between the weight of the lifted soil and the friction on the blade surface. In fact, for low rake angles the weight is greater than the friction force component, at 75° they are equal (RF2 = 0), then the opposite occurs.

To validate the finite element model results, they have been compared to the experimental investigations of Chi & Kushwaha (1990) using a soil bin. Indeed, the same experimental conditions have been investigated in a numerical model (Table 2). Fig. 8b shows similar trends of the predicted forces (vertical and draught) with the experimental curves.

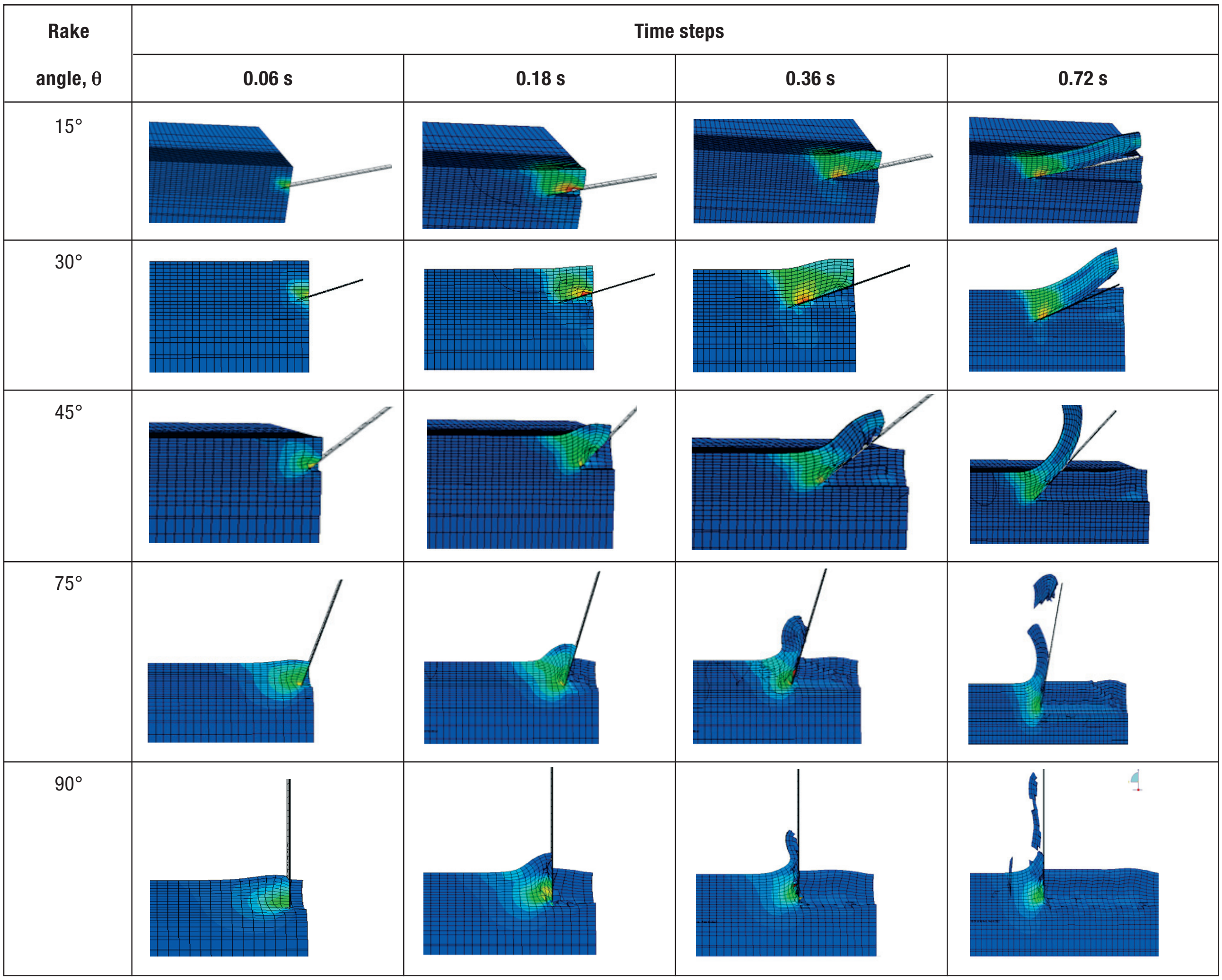

Figure 7. Cutting process of the blade at different time steps *versus* the rake angle (θ).

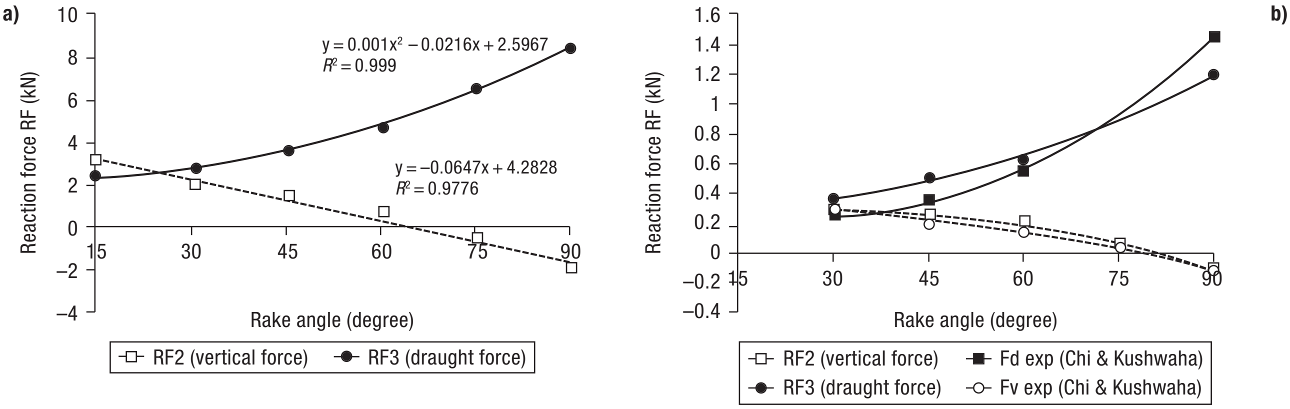

Figure 8. (a) Effect of the rake angle on the tillage forces (a) and comparison of obtained numerical results with experimental forces of Chi & Kushwaha (1990) (b). Draught force (Fd, RF3); vertical force (Fv, RF2).

Table 2. Mechanical properties of the soil bin used in the experimental investigations of Chi & Kushwaha (1990)

Parameters	Value
Density, ρ (kgm^{-3})	1,434
Adhesion, *Ca* (kPa)	3.29
Friction coefficient angle, ϕ (degree)	34.5
Cohesion, *C* (kPa)	7.19
Soil-metal friction angle, δ (degree)	23.5
Depth, *d* (m)	0.1
Width, *w* (m)	0.05

Effect of the cutting angle (θ = 90°)

Fig. 9 shows the cutting process at t = 0.72 s for different cutting angles (α). For a small cutting angle of 15° the tool slips into the soil, then from 30° to 60° the soil is cut and reversed to the right side of the blade. For high angles (75° to 90°), the soil is reversed in front of the blade.

The mean value of the obtained forces after stabilization, for each angle, is drawn in Fig. 10a in order to present the variability of the different forces *versus* the cutting angle. These curves demonstrate that both,

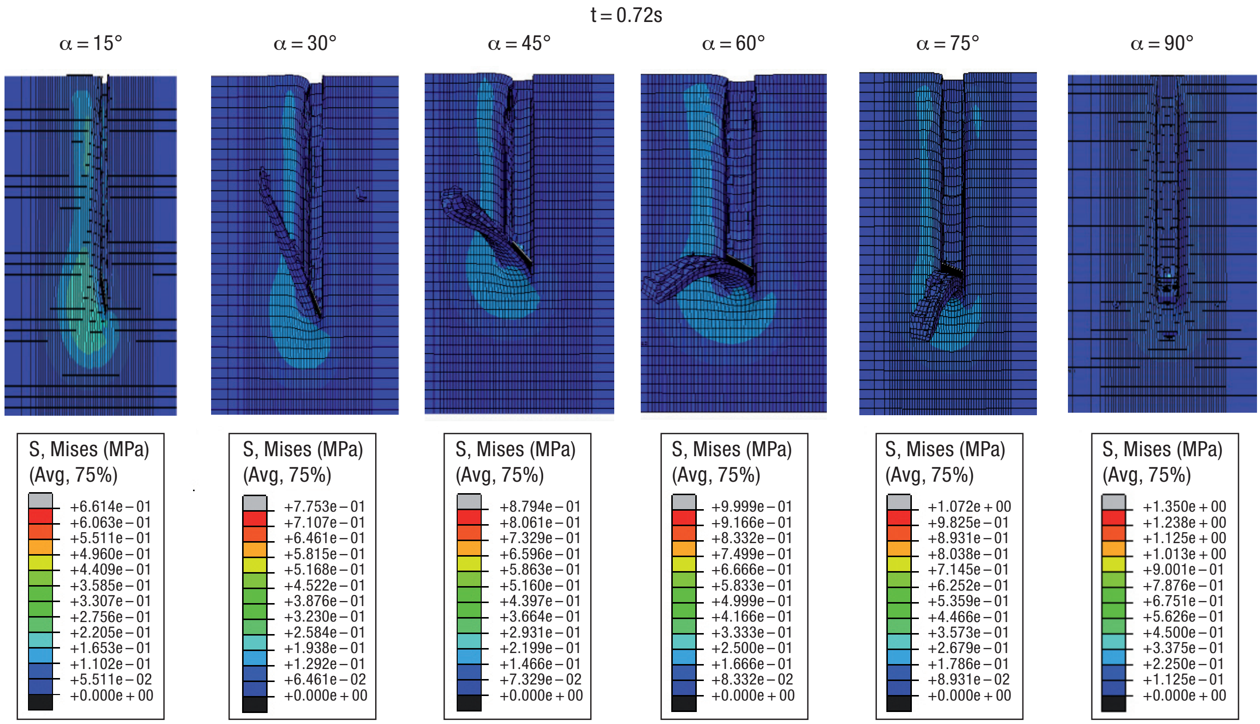

Figure 9. Cutting proccess for different cutting angles at time step t = 0.72 s.

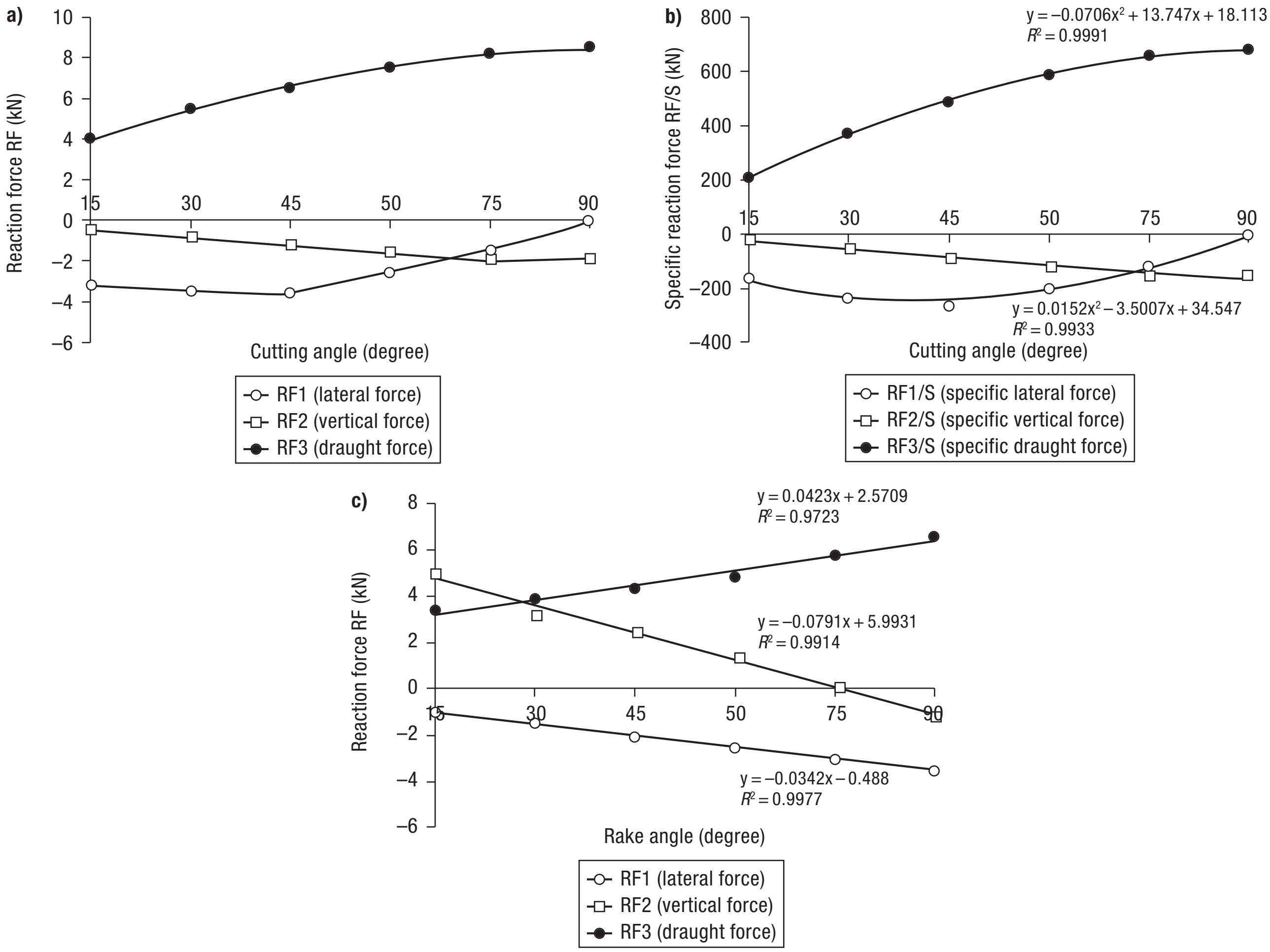

Figure 10. Case of the inclined blade: effect of the cutting angle on tillage forces (a) and specific forces (b), and the rake angle on the tillage forces (c). $\alpha = 45$ degrees.

draught and vertical forces, increase when the cutting angle increases. However, the lateral force presents a maximum value for a cutting angle of 45°. The draught force presents the highest values compared to the vertical and lateral forces. Taking into consideration the attack surface of the blade to calculate specific forces, the specific draught presents a polynomial variation with the maximum at 90° (Fig. 10b).

The specific lateral force presents a polynomial function with a maximum of 262 kPa at $\alpha = 45°$. The specific vertical force increases linearly with a low slope with an increasing cutting angle.

Effect of the rake angle (α = 45°)

An important effect of the rake angle (θ) on the tillage forces was found in the previous study for a cutting angle fixed at 90°. In this part of the study an oblique orientation of the tool (see Fig. 1) is considered to be close to the moldboard cutting process. The blade was oriented with a fixed cutting angle equal to 45° and different rake angles (15°, 30°, 45°, 60°, 75°, and 90°) were studied. Fig. 10c shows that the draught and lateral forces increase when the rake angle increases linearly. The vertical force decreases linearly until becoming negative ($\theta > 75°$). This result is similar to that reached with the previous case ($\alpha = 90°$).

In summary, in this work a numerical model of the tillage process with a cutting blade was developed with the finite element method (FEM) using the linear form of the Drucker-Prager model. A subroutine for mesh failure was introduced to Abaqus Explicit software. First, the effects of the tillage depth and of the tool width were investigated. Then, the influence of the cutting angle (α) and the rake or lifting angle (θ) were studied through the three components of the predicted tillage force. In fact, the soil in front of the blade slips, is reversed or fragmented respectively to low, medium and high rake angles. These results prove that a single equation cannot describe these difficult behaviors of the soil. The cutting angle (α) determines the orientation of the cut soil after its failure. These studies showed that working with higher width and depth increased the consumed energy which directly related to the draught force (Mouazen & Nemeny, 1999). A good soil inversion can be achieved when fixing the blade with small cutting angle and an average rake angle (30° to 60° and 45° respectively).

Acknowledgements

The authors wish to thank the members of the electromechanical systems laboratory at the National Engineering School of Sfax University for supporting this research.

References

Abaqus, 2010. Abaqus user's manuals, vers. 6.10.1. Abaqus Inc, Providence, RI, USA.

Abo-Elnor M, Hamilton R, Boyle JT, 2004. Simulation of soil-blade interaction for sandy soil using advanced 3D finite element analysis. Soil Till Res 75: 61-73.

Bentaher H, Ibrahmi A, Hamza E, Hbaieb M, Kantchev G, Maalej A, Arnold W, 2013.Finite element simulation of moldboard-soil interaction. Soil Till Res 134: 11-16.

Bloome PD, Batchelder DG, Khalilian A, Riethmuller GP, 1983. Effects of speed on draft of tillage implements in Oklahoma soils. ASAE Paper No 83-1032. St Joseph, MI, USA.

Bose SK, Som NN, 1998. Parametric study of a braced cut by finite element method. Comput Geotechn 22(2): 91-107.

Celik A, Altikat S, Way TR, 2013.Strip tillage width effects on sunflower seed emergence and yield. Soil Till Res 131: 20-27.

Chen Y, Munkholm LJ, Nyord T, 2013. A discrete element model for soil-sweep interaction in three different soils. Soil Till Res 126: 34-41.

Chi L, Kushwaha RL, 1987. Three dimensional finite element analysis of soil failure under a narrow tillage tool. ASAE Paper No 88-1582, St Joseph, MI, USA.

Chi L, Kushwaha RL, 1988. Finite element analysis of soil forces in tillage. Can Soc Agric Eng, Paper No 88-205.

Chi L, Kushwaha RL, 1990. A non-linear 3-d finite element analysis of soil failure with tillage tools. J Terramechanics 27(4): 343-366.

Collins NE, Kemble LJ, Williams TH, Handy WE, 1978. Energy requirements for tillage on coastal plains soils. ASAE Paper No 78-1517. St Joseph, MI, USA.

Davoudi S, Alimardani R, Keyhani A, Atarnejad R, 2008. A two dimensional finite element analysis of a plane tillage tool in soil using a non-linear elasto-plastic model. Am-Euras J Agric Environ Sci 3(3): 498-505.

Fielke JM, 1999. Finite element modelling of the interaction of the cutting edge of tillage implements with soil. J Agr Eng Res 74: 91-101.

FrancoY, Rubinstein D, Shmulevich I, 2007. Prediction of soil-bulldozer blade interaction using discrete element method. T Am Soc Agr Biol Eng 50(2): 345-353.

Godwin RJ, O'Dogherty MJ, 2007. Integrated soil tillage force prediction models. J Terramechanics 44(1): 3-14.

Gupta PD, Gupta CP, Pandey KP, 1989. An analytical model for predicting draft forces on convex-type wide cutting blades. Soil Till Res 14: 131-144.

Karmakar S, Kushwaha RL, 2005. Simulation of soil deformation around a tillage tool using computational fluid dynamics. T ASAE 48(3): 923-932.

Karmakar S, Kushwaha RL, Lague C, 2007. Numerical modelling of soil stress and pressure distribution on a flat tillage tool using computational fluid dynamics. Biosyst Eng 97(3): 407-414.

Karmakar S, Ashrafizadeh SR, Kushwaha RL, 2009. Experimental validation of computational fluid dynamics modeling for narrow tillage tool draft. J Terramechanics 46: 277-283.

Li GX, 2004. Advanced soil mechanics. The Tsinghua University Press, Beijing. [In Chinese].

Licht MA, Al-Kaisi M, 2005. Strip-tillage effect on seedbed soil temperature and other soil physical properties. Soil Till Res 80(1-2): 233-249.

Manuwa SI, 2009. Performance evaluation of tillage tines operating under different depths in a sandy clay loam soil. Soil Till Res 103: 399-405.

McKyes E, Ali OS, 1977. The cutting of soil by narrow blades. J Terramechanics 14(2): 43-58.

Mckyes E, Desir FL, 1984. Prediction and field measurements of tillage tool draft forces and efficiency in cohesive soils. Soil Till Res 4: 459-470.

Momozu M, Oida A, Yamazaki M, Koolen AJ, 2003. Simulation of a soil loosening process by means of the modified distinct element method. J Terramechanics 39: 207-220.

Mouazen AM, Nemenyi M, 1999. Finite element analysis of subsoiler cutting in non-homogeneous sandy loam soil. Soil Till Res 51: 1-15.

Mullins GL, Alley SE, Reeves DW, 1998.Tropical maize response to nitrogen and starter fertilizer under strip and conventional tillage systems in southern Alabama. Soil Till Res 45 (1-2): 1-15.

Obermayr M, Dressler K, Vrettos C, Eberhard P, 2011. Prediction of draft forces in cohesionless soil with the discrete element method. J Terramechanics 48(5): 347-358.

Owend PMO, Eward SM, 1996. Characteristic loading of light mouldboard ploughs at slow speeds. J Terramechanics 335(1): 29-53.

Richards BG, Peth S, 2009. Modelling soil physical behaviour with particular reference to soil science. Soil Till Res 102: 216-224.

Shmulevich I, Asaf Z, Rubinstein D, 2007. Interaction between soil and a wide cutting blade using the discrete element method. Soil Till Res 97: 37-50.

Shmulevich I, 2010. State of the art modeling of soil-tillage interaction using discrete element method. Soil Till Res 111(1): 41-53.

Singh N, Singh G, Salokhe VM, 1991. Cyclic variation in moldboard plow draft and its effect on implement control systems. Soil Till Res 21: 273-286.

Tamas K, Jori IJ, Mouazen AM, 2013. Modelling soil-sweep interaction with discrete element method. Soil Till Res 134: 223-231.

Temesgen M, Rockstrom J, Savenije HHG, Hoogmoed WB, Alemu D, 2008. Determinants of tillage frequency among small holder farmers in two semi-arid areas in Ethiopia. Physics and Chemistry of the Earth, Parts A/B/C 33(1-2): 183-191.

Temesgen M, Savenije HHG, Rockström J, Hoogmoed WB, 2012. Assessment of strip tillage systems for maize production in semi-arid Ethiopia: effects on grain yield, water balance and water productivity. Physics and Chemistry of the Earth, Parts A/B/C 47-48: 156-165.

Tong J, Moayad BZ, 2006. Effects of rake angle of chisel plough on soil cutting factors and power requirements: a computer simulation. Soil Till Res 88: 55-64.

Trevini M, Benincasa P, Guiducci M, 2013. Strip tillage effect on seedbed tilth and maize production in Northern Italy as case-study for the Southern Europe environment. Eur J Agron 48: 50-56.

Ucgul M, Fielke JM, Saunders C, 2014. Three-dimensional discrete element modelling of tillage: determination of a suitable contact model and parameters for a cohesionless soil. Biosyst Eng 121: 105-117.

Upadhyaya SK, Rosa UA, Wulfsohn D, 2002. Application of the finite element method in agricultural soil mechanics. Adv Soil Dynamics 2: 117-153.

Yong RN, Hanna AW, 1977. Finite element analysis of plane soil cutting. J Terramechanics 14(3): 103-125.

Zhang XY, 1993. Geotechnical plastic mechanics. China Communications Press, Beijing. [In Chinese].